Control of Hamiltonian chaos as a possible tool to control anomalous transport in fusion plasmas

Guido Ciraolo*
Facoltà di Ingegneria, Università di Firenze, via S. Marta, I-50129 Firenze, Italy
and INFM UdR Firenze, Firenze, Italy

Françoise Briolle,[†] Cristel Chandre,[‡] Elena Floriani,[§] Ricardo Lima,[‖] and Michel Vittot[¶]
CPT-CNRS, Luminy Case 907, F-13288 Marseille Cedex 9, France

Marco Pettini**
Istituto Nazionale di Astrofisica, Osservatorio Astrofisico di Arcetri, Largo Enrico Fermi 5, I-50125 Firenze, Italy,
and INFM UdR Firenze and INFN Sezione di Firenze, Firenze, Italy

Charles Figarella[††] and Philippe Ghendrih[‡‡]
Association Euratom-CEA, DRFC/DSM/CEA, CEA Cadarache, F-13108 St. Paul-lez-Durance Cedex, France

It is shown that a relevant control of Hamiltonian chaos is possible through suitable small perturbations whose form can be explicitly computed. In particular, it is possible to control (reduce) the chaotic diffusion in the phase space of a Hamiltonian system with 1.5 degrees of freedom which models the diffusion of charged test particles in a turbulent electric field across the confining magnetic field in controlled thermonuclear fusion devices. Though still far from practical applications, this result suggests that some strategy to control turbulent transport in magnetized plasmas, in particular, tokamaks, is conceivable. The robustness of the control is investigated in terms of a departure from the optimum magnitude, of a varying cutoff at large wave vectors, and of random errors on the phases of the modes. In all three cases, there is a significant region of maximum efficiency in the vicinity of the optimum control term.

I. INTRODUCTION

Transport induced by chaotic motion is now a standard framework to analyze the properties of numerous systems. Since chaos can be harmful in several contexts, during the last decade or so, much attention has been paid to the so-called topic of *chaos control*. Here the meaning of *control* is that one aims at reducing or suppressing chaos inducing a relevant change in the transport properties, by means of a small perturbation (either open-loop or closed-loop control of dissipative systems [1,2]) so that the original structure of the system under investigation is substantially kept unaltered. Control of *chaotic transport* properties still remains an open issue with considerable applications.

In the case of dissipative systems, an efficient strategy of control works by stabilizing unstable periodic orbits, where the dynamics is eventually attracted. Similarly, a first idea to control Hamiltonian systems is to modify the parameters of the system in order to act on periodic orbits: One can enhance the stability of elliptic periodic orbits by zeroing their residues [3] or by stabilizing hyperbolic periodic orbits [4].

Another idea to stabilize the system is to enlarge the phase space by coupling the system with an external system (and hence with additional degrees of freedom which makes the large system more regular) [5]. These embedding techniques are similar to the above methods on the stabilization of unstable periodic orbits; they are based on the construction of a dissipative system from the original Hamiltonian system. The techniques developed for dissipative systems can thus be applied to this modified system, such as, for instance, the targeting of periodic orbits.

A different approach is to modify the Hamiltonian (or just the potential) to control the original system. This approach is useful when one is able to act on this system with an external force. The interesting point is that the Hamiltonian structure with its number of degrees of freedom is preserved. So far, the modifications of the Hamiltonian that have been proposed in the literature are the following: the modification of the integrable part of the Hamiltonian [6], the control of a system with large and nonsmooth external pulses [7], a localized control with a modification in some specific regions of phase space [8], or a control using variations of the external field [9,10]. However, we notice that most of the modifications of the potential that have been proposed so far are tailored to specific examples (with the exception of the optimal control [9]) and the required modifications are large compared with the potential.

*Electronic address: ciraolo@arcetri.astro.it
[†]Electronic address: briolle@cpt.univ-mrs.fr
[‡]Electronic address: chandre@cpt.univ-mrs.fr
[§]Electronic address: floriani@cpt.univ-mrs.fr
[‖]Electronic address: lima@cpt.univ-mrs.fr
[¶]Electronic address: vittot@cpt.univ-mrs.fr
**Electronic address: pettini@arcetri.astro.it
[††]Electronic address: charles.figarella@cea.fr
[‡‡]Electronic address: philippe.ghendrih@cea.fr

Hamiltonian description of the microscopic origin of particle transport usually involves a large number of particles. Methods based on targeting and locking to islands of regular motions in a "chaotic sea" are of no practical use for controlling when dealing simultaneously with a large number of unknown trajectories. Therefore, the most efficient procedure appears to be to control the transport process with a small perturbation, if any, making the system integrable or closer to integrable. In what follows we show that it is actually possible to control Hamiltonian chaos in this way by preserving the Hamiltonian structure. We describe a general method for controlling nearly integrable Hamiltonian systems, and we apply this technique to a model relevant to magnetized plasmas.

Chaotic transport of particles advected by a turbulent electric field with a strong magnetic field is associated with Hamiltonian dynamical systems under the approximation of the guiding center motion due to $\mathbf{E} \times \mathbf{B}$ drift velocity. For an appropriate choice of the turbulent electric field, it has been shown that the resulting diffusive transport is then found to agree with the experimental counterpart [11]. It is clear that such an analysis is only a first step in the investigation and understanding of turbulent plasma transport. The control of transport in magnetically confined plasmas is of major importance in the long way to achieve controlled thermonuclear fusion. Two major mechanisms have been proposed for such a turbulent transport: transport governed by the fluctuations of the magnetic field and transport governed by fluctuations of the electric field. There is presently a general consensus to consider, at low plasma pressure, that the latter mechanism agrees with experimental evidence [12]. In the area of transport of trace impurities, i.e., that are sufficiently diluted so as not to modify the electric field pattern, the $\mathbf{E} \times \mathbf{B}$ drift motion of test particle should be the exact transport model. Even for this very restricted case, control of chaotic transport would be very relevant for the thermonuclear fusion program. The possibility of reducing and even suppressing chaos combined with the empirically found states of improved confinement in tokamaks suggest to investigate the possibility to devise a strategy of control of chaotic transport through some smart perturbations acting at the microscopic level of charged particle motions.

As in the current literature the electric turbulent transport in plasmas is mainly addressed in the Eulerian (fluid) framework, let us first recall the difference between Lagrangian and Eulerian descriptions of transport. We consider the advection of a scalar quantity $\theta(\mathbf{x},t)$ describing, e.g., the concentration of a passively transported entity. In a given Eulerian velocity field $\mathbf{v}(\mathbf{x},t)$ the transport of $\theta(\mathbf{x},t)$ is described by

$$\frac{\partial \theta(\mathbf{x},t)}{\partial t} + \mathbf{v}(\mathbf{x},t) \cdot \boldsymbol{\nabla} \, \theta(\mathbf{x},t) = D\nabla^2 \theta(\mathbf{x},t), \qquad (1.1)$$

where D is a molecular diffusion coefficient. This equation holds for both neutral fluids and plasmas. If the field $\mathbf{v}(\mathbf{x},t)$ is given independently from the field $\theta(\mathbf{x},t)$, Eq. (1.1) is linear in $\mathbf{v}(\mathbf{x},t)$. The complexity of the field $\theta(\mathbf{x},t)$ will then depend on both the complexity of the field $\mathbf{v}(\mathbf{x},t)$ and on the

molecular diffusion coefficient D. When considering the simulation of Eq. (1.1), the magnitude of D will govern the mesh size to store the field $\theta(\mathbf{x},t)$. For a vanishingly small diffusion D, there will be no cutoff of the small scales generated by the simulation. This will require an infinite storage capability to describe the complexity of $\theta(\mathbf{x},t)$ that can appear even for a relatively smooth velocity field. To evaluate this property, the most straightforward description is given by a Lagrangian approach. For the same transport process, the latter requires to solve the following equations of motion of a passive tracer (e.g., particle, fluid drop) whose Eulerian concentration function is $\theta(\mathbf{x},t)$,

$$\dot{\mathbf{x}} = \mathbf{v}(\mathbf{x},t), \qquad (1.2)$$

which in the case of a two-dimensional incompressible Euler flow can be given by the form

$$\dot{\mathbf{x}} = \frac{d}{dt}\begin{pmatrix} x \\ y \end{pmatrix} = \mathbf{v}(\mathbf{x},t) = \boldsymbol{\nabla}^{\perp}\psi = \begin{pmatrix} -\partial_y \psi(x,y,t) \\ \partial_x \psi(x,y,t) \end{pmatrix}, \quad (1.3)$$

where ψ denotes the stream function of the Eulerian field $\mathbf{v}(\mathbf{x},t)$, the trajectory of the tracer is denoted by $\mathbf{x}(t)$, and $\boldsymbol{\nabla}^{\perp} \equiv (-\partial_y, \partial_x)$. What is remarkable here is the Hamiltonian structure of the equations of motion (1.3), where the stream function ψ plays the role of the Hamiltonian function and x and y play the role of the canonically conjugate variables. With the exception of trivial velocity fields $\mathbf{v}$ (such as a uniform, parallel flow) these equations of motion are in general nonlinear in the coordinates; in fact, if we even think of a simple vortex, we realize that v_x and v_y must contain at least one trigonometric function. Now, also without a standard (quadratic) kinetic energy term, this kind of Hamiltonian dynamical system displays all the rich and complex phenomenology of the transition between regular and chaotic motions and between weak and strong chaos [13]. Thus, even in the presence of rather regular Eulerian velocity patterns, the solutions of Eqs. (1.2) and (1.3) can be very complicated, with apparently no relation left with $\mathbf{v}(\mathbf{x},t)$. In other words, chaotic Lagrangian diffusion can take place also in the presence of rather simple Eulerian velocity patterns. For realistic simulation of Eq. (1.1) a finite mesh size must be introduced and accordingly the diffusion coefficient D must reach a finite value to smear out the small scales that cannot be captured by the grid. If the velocity field is characterized by a large regular structure superimposed to small scale structures, the output of the simulation can lead to the absence of any diffusion but the molecular one [14]. The difficulty in the simulation of Eq. (1.1) will then lead to an apparent conflict with a broad experimental evidence [15]. The most efficient means to address the transport of passive scalars in a given velocity field $\mathbf{v}(\mathbf{x},t)$ appears to follow a Lagrangian approach that allows one to describe the motion at all scales in space and time. The cost of this method will appear in the statistics that must be performed to obtain a general property of the system whenever a single trajectory does not allow one to capture the properties of all possible trajectories.

When addressing plasma transport, Eulerian and Lagrangian approaches are combined to provide an analysis of the transport properties. An equation similar to Eq. (1.1) is coupled to a vorticity equation defining the field $\mathbf{v}(\mathbf{x},t)$ [16]. The Eulerian description is used to generate the velocity field and a Lagrangian approach is used to follow trace impurities and trace tritium that allows one to compare the simulations to experimental data [17].

A close analogy exists between the equations of motion of passive tracers (1.3) and those of the guiding centers of charged particles moving in strongly magnetized plasmas and in the presence either of an electric field transverse to the magnetic field or of an inhomogeneous component of the magnetic field itself. The electrostatic case [18] is modeled by

$$\dot{\mathbf{x}} = \frac{d}{dt}\begin{pmatrix} x \\ y \end{pmatrix} = \frac{c}{B^2}\mathbf{E}(\mathbf{x},t) \times \mathbf{B} = \frac{c}{B}\begin{pmatrix} -\partial_y V(x,y,t) \\ \partial_x V(x,y,t) \end{pmatrix},$$

where V is the electric potential, $\mathbf{E} = -\boldsymbol{\nabla}V$, and $\mathbf{B} = B\mathbf{e}_z$. The magnetic case is modeled by

$$\dot{\mathbf{x}} = \frac{d}{dt}\begin{pmatrix} x \\ y \end{pmatrix} = \frac{\mathbf{v}_\parallel}{RB} \times \boldsymbol{\nabla}\,\Phi_{pol}(\mathbf{x},t) = \frac{v_\parallel}{RB}\begin{pmatrix} -\partial_y \Phi_{pol}(x,y,t) \\ \partial_x \Phi_{pol}(x,y,t) \end{pmatrix},$$

(1.4)

where $\mathbf{v}_\parallel$ is the velocity along the field line, R the major radius of the torus, and Φ_{pol} the poloidal magnetic flux divided by 2π. In both cases, the physically remarkable phenomenon—in complete analogy with the Lagrangian diffusion of passive scalars—is that even in the presence of rather regular space-time patterns of the electric fields or of the magnetic inhomogeneities, the charged particles can diffuse across the magnetic field which ceases to be confining. The dynamical instability with respect to small variations of the initial conditions, known as deterministic chaos, is the very source of the enhanced cross-field diffusion; it is "intrinsically" noncollisional and it turns out to be orders of magnitude larger than the collisional one [11], sometimes even many orders of magnitude larger [19].

In this paper, the problem we address is how to control chaotic diffusion in such Hamiltonian models. In some range of parameters, the problems can be considered as nearly integrable. We consider the class of Hamiltonian systems which can be written in the form $H = H_0 + \epsilon V$ that is an integrable Hamiltonian H_0 (with action-angle variables) plus a small perturbation ϵV.

The problem of control in Hamiltonian systems is the following one: For the perturbed Hamiltonian $H_0 + \epsilon V$, the aim is to devise a control term f such that the dynamics of the controlled Hamiltonian $H_0 + \epsilon V + f$ has more regular trajectories (e.g., on invariant tori) or less diffusion than the uncontrolled one. Obviously $f = -\epsilon V$ is a solution since the resulting Hamiltonian is integrable. However, it is a useless solution since the control is of the same magnitude as of the perturbation. For practical purposes, the desired control term should be small (with respect to the perturbation ϵV), localized in phase space (meaning that the subset of phase space

where f is nonzero is finite or small enough), or f should be of a specific shape (e.g., a sum of given Fourier modes or with a certain regularity). Moreover, the control should be as simple as possible in view of future implementations in experiments.

In Sec. II, we explain the control theory of nearly integrable Hamiltonian systems following Ref. [20]. We show that it is possible to construct and compute analytically a control term f of order ϵ^2 such that the controlled Hamiltonian $H_c = H_0 + \epsilon V + f$ is integrable. In Sec. III, after defining the model of interest to our study in Sec. III A, we compute analytically the first terms of the expansion of the control term in Sec. III B. Some properties of the control term are given in Sec. III C. A numerical study of the effect of the control term on the dynamics is done extensively in Sec. IV. It is shown that the chosen control term is able to drastically reduce the chaotic transport. In Sec. V, we study the effect of some truncations that aim at either simplifying the control term or reducing the energy input to control the system: In particular, we show that reducing the control term to its main Fourier components or reducing the magnitude of the control term is sufficient to govern a significant decrease of the chaotic transport. Though, of course the optimal control is obtained with the full control term. These results indicate that this control of Hamiltonian systems is robust.

II. CONTROL THEORY OF HAMILTONIAN SYSTEMS

In this section, following the framework of Ref. [20] we explain the control theory of Hamiltonian systems. Let $\mathcal{A}$ be the vector space of C^∞ real functions defined on the phase space. For $H \in \mathcal{A}$, let $\{H\}$ be the linear operator acting on $\mathcal{A}$ such that

$$\{H\}H' = \{H,H'\},$$

for any $H' \in \mathcal{A}$, where $\{\cdot,\cdot\}$ is the Poisson bracket. Hence $\mathcal{A}$ is a Lie algebra. The time evolution of a function $V \in \mathcal{A}$ following the flow of H is given by

$$\frac{dV}{dt} = \{H\}V,$$

which is formally solved as

$$V(t) = e^{t\{H\}}V(0),$$

if H is time independent, and where

$$e^{t\{H\}} = \sum_{n=0}^{\infty} \frac{t^n}{n!}\{H\}^n.$$

Any element $V \in \mathcal{A}$ such that $\{H\}V = 0$ is constant under the flow of H, i.e.,

$$\forall t \in \mathbb{R}, \quad e^{t\{H\}}V = V.$$

Let us now consider a given Hamiltonian $H_0 \in \mathcal{A}$. The operator $\{H_0\}$ is not invertible since a derivation has always a nontrivial kernel. For instance, $\{H_0\}H_0{}^\alpha = 0$ for any α such that $H_0{}^\alpha \in \mathcal{A}$. The vector space $\mathrm{Ker}\{H_0\}$ is the set of constants of motion. Hence we consider a pseudoinverse of

$\{H_0\}$. We define a linear operator Γ on $\mathcal{A}$ such that

$$\{H_0\}^2\Gamma = \{H_0\}, \tag{2.1}$$

i.e.,

$$\forall V \in \mathcal{A}, \quad \{H_0, \{H_0, \Gamma V\}\} = \{H_0, V\}.$$

The operator Γ is not unique. Any other choice of Γ' satisfies that the range $\mathrm{Rg}(\Gamma' - \Gamma)$ is included into the kernel $\mathrm{Ker}(\{H_0\}^2)$.

We define the *nonresonant* operator $\mathcal{N}$ and the *resonant* operator $\mathcal{R}$ as

$$\mathcal{N} = \{H_0\}\Gamma,$$

$$\mathcal{R} = 1 - \mathcal{N},$$

where the operator 1 is the identity in the algebra of linear operators acting on $\mathcal{A}$. We notice that Eq. (2.1) becomes

$$\{H_0\}\mathcal{R} = 0,$$

which means that the range $\mathrm{Rg}\,\mathcal{R}$ of the operator $\mathcal{R}$ is included in $\mathrm{Ker}\{H_0\}$. A consequence is that $\mathcal{R}V$ is constant under the flow of H_0, i.e., $e^{t\{H_0\}}\mathcal{R}V = \mathcal{R}V$. We notice that when $\{H_0\}$ and Γ commute, $\mathcal{R}$ and $\mathcal{N}$ are projectors, i.e., $\mathcal{R}^2 = \mathcal{R}$ and $\mathcal{N}^2 = \mathcal{N}$. Moreover, in this case we have $\mathrm{Rg}\,\mathcal{R} = \mathrm{Ker}\{H_0\}$, i.e., the constant of motion are the elements $\mathcal{R}V$ where $V \in \mathcal{A}$.

Let us now assume that H_0 is integrable with action-angle variables $(\mathbf{A}, \boldsymbol{\varphi}) \in \mathcal{B} \times \mathbb{T}^l$ where $\mathcal{B}$ is an open set of $\mathbb{R}^l$ and $\mathbb{T}^l$ is the l-dimensional torus. Thus $H_0 = H_0(\mathbf{A})$ and the Poisson bracket $\{H, H'\}$ between two elements H and H' of $\mathcal{A}$ is

$$\{H, H'\} = \frac{\partial H}{\partial \mathbf{A}} \cdot \frac{\partial H'}{\partial \boldsymbol{\varphi}} - \frac{\partial H}{\partial \boldsymbol{\varphi}} \cdot \frac{\partial H'}{\partial \mathbf{A}}.$$

The operator $\{H_0\}$ acts on V expanded as follows:

$$V = \sum_{\mathbf{k} \in \mathbb{Z}^l} V_{\mathbf{k}}(\mathbf{A}) e^{i\mathbf{k} \cdot \boldsymbol{\varphi}},$$

as

$$\{H_0\}V(\mathbf{A}, \boldsymbol{\varphi}) = \sum_{\mathbf{k}} i\boldsymbol{\omega}(\mathbf{A}) \cdot \mathbf{k} \quad V_{\mathbf{k}}(\mathbf{A}) e^{i\mathbf{k} \cdot \boldsymbol{\varphi}},$$

where

$$\boldsymbol{\omega}(\mathbf{A}) = \frac{\partial H_0}{\partial \mathbf{A}}.$$

A possible choice of Γ is

$$\Gamma V(\mathbf{A}, \boldsymbol{\varphi}) = \sum_{\substack{\mathbf{k} \in \mathbb{Z}^l \\ \boldsymbol{\omega}(\mathbf{A}) \cdot \mathbf{k} \neq 0}} \frac{V_{\mathbf{k}}(\mathbf{A})}{i\boldsymbol{\omega}(\mathbf{A}) \cdot \mathbf{k}} e^{i\mathbf{k} \cdot \boldsymbol{\varphi}}. \tag{2.2}$$

We notice that this choice of Γ commutes with $\{H_0\}$.

For a given $V \in \mathcal{A}$, $\mathcal{R}V$ is the resonant part of V and $\mathcal{N}V$ is the nonresonant part:

$$\mathcal{R}V = \sum_{\mathbf{k}} V_{\mathbf{k}}(\mathbf{A})\chi(\boldsymbol{\omega}(\mathbf{A}) \cdot \mathbf{k} = 0) e^{i\mathbf{k} \cdot \boldsymbol{\varphi}}, \tag{2.3}$$

$$\mathcal{N}V = \sum_{\mathbf{k}} V_{\mathbf{k}}(\mathbf{A})\chi(\boldsymbol{\omega}(\mathbf{A}) \cdot \mathbf{k} \neq 0) e^{i\mathbf{k} \cdot \boldsymbol{\varphi}}, \tag{2.4}$$

where $\chi(\alpha = 0)$ vanishes when $\alpha \neq 0$ and it is equal to 1 when $\alpha = 0$.

From these operators defined for the integrable part H_0, we construct a control term for the perturbed Hamiltonian $H_0 + V$ where $V \in \mathcal{A}$, i.e., f is constructed such that $H_0 + V + f$ is canonically conjugate to $H_0 + \mathcal{R}V$.

Proposition 1. For $V \in \mathcal{A}$ and Γ constructed from H_0, we have the following equation:

$$e^{\{\Gamma V\}}(H_0 + V + f) = H_0 + \mathcal{R}V, \tag{2.5}$$

where

$$f(V) = e^{-\{\Gamma V\}}\mathcal{R}V + \frac{1 - e^{-\{\Gamma V\}}}{\{\Gamma V\}}\mathcal{N}V - V. \tag{2.6}$$

We notice that the operator $(1 - e^{-\{\Gamma V\}})/\{\Gamma V\}$ is well defined by the expansion

$$\frac{1 - e^{-\{\Gamma V\}}}{\{\Gamma V\}} = \sum_{n=0}^{\infty} \frac{(-1)^n}{(n+1)!}\{\Gamma V\}^n.$$

Proof. Since $e^{\{\Gamma V\}}$ is invertible, Eq. (2.5) gives

$$f(V) = (e^{-\{\Gamma V\}} - 1)H_0 + e^{-\{\Gamma V\}}\mathcal{R}V - V.$$

We notice that the operator $e^{-\{\Gamma V\}} - 1$ can be divided by $\{\Gamma V\}$,

$$f(V) = \frac{e^{-\{\Gamma V\}} - 1}{\{\Gamma V\}}\{\Gamma V\}H_0 + e^{-\{\Gamma V\}}\mathcal{R}V - V.$$

By using the relations

$$\{\Gamma V\}H_0 = \{\Gamma V, H_0\} = -\{H_0\}\Gamma V$$

and

$$\{H_0\}\Gamma = \mathcal{N},$$

we have

$$f(V) = e^{-\{\Gamma V\}}\mathcal{R}V + \frac{1 - e^{-\{\Gamma V\}}}{\{\Gamma V\}}\mathcal{N}V - V. \qquad \square$$

The control term can be expanded in power series as

$$f(V) = \sum_{n=1}^{\infty} \frac{(-1)^n}{(n+1)!}\{\Gamma V\}^n(n\,\mathcal{R} + 1)V. \tag{2.7}$$

We notice that if V is of order ϵ, $f(V)$ is of order ϵ^2.

Proposition 1 tells that the addition of a well chosen control term f makes the Hamiltonian canonically conjugate to $H_0 + \mathcal{R}V$. It is also possible to show from Proposition 1 that the flow of $H_0 + V + f$ is conjugate to the flow of $H_0 + \mathcal{R}V$ (see Ref. [20]).

Proposition 2.

$$\forall t \in \mathbb{R}, \quad e^{t\{H_0+V+f\}} = e^{-\{\Gamma V\}} \quad e^{t\{H_0\}} \quad e^{t\{RV\}} \quad e^{\{\Gamma V\}}.$$

The remarkable fact is that the flow of $\mathcal{R}V$ commutes with the one of H_0, since $\{H_0\}\mathcal{R}=0$. This allows the splitting of the flow of $H_0+\mathcal{R}V$ into a product.

The notion of nonresonant Hamiltonian is defined by the following statement.

Definition. H_0 is nonresonant if and only if $\forall \mathbf{A} \in \mathcal{B}, \boldsymbol{\omega}(\mathbf{A}) \cdot \mathbf{k} = 0$ implies $\mathbf{k} = \mathbf{0}$.

If H_0 is nonresonant then with the addition of a control term f, the Hamiltonian H_0+V+f is canonically conjugate to the integrable Hamiltonian $H_0+\mathcal{R}V$ since $\mathcal{R}V$ is only a function of the actions [see Eq. (2.3)].

If H_0 is resonant and $\mathcal{R}V=0$, the controlled Hamiltonian $H=H_0+V+f$ is conjugate to H_0.

In the case $\mathcal{R}V=0$, the series (2.7), which gives the expansion of the control term f, can be written as

$$f(V) = \sum_{s=2}^{\infty} f_s, \tag{2.8}$$

where f_s is of order ϵ^s and given by the recursion formula

$$f_s = -\frac{1}{s}\{\Gamma V, f_{s-1}\}, \tag{2.9}$$

where $f_1=V$.

Remark. A different approach of control has been developed by Gallavotti in Ref. [6]. The idea is to find a control term (named *counter term*) depending only on the actions, i.e., to find N such that

$$H(\mathbf{A}, \boldsymbol{\varphi}) = H_0(\mathbf{A}) + V(\mathbf{A}, \boldsymbol{\varphi}) - N(\mathbf{A})$$

is integrable. For isochronous systems, that is,

$$H_0(\mathbf{A}) = \boldsymbol{\omega} \cdot \mathbf{A},$$

or any function $h(\boldsymbol{\omega}\cdot\mathbf{A})$, it is shown that if the frequency vector satisfies a Diophantine condition and if the perturbation is sufficiently small and smooth, such a control term exists. An algorithm to compute it by recursion is provided by the proof. We notice that the resulting control term N is of the same order as the perturbation, and has the following expansion:

$$N(\mathbf{A}) = \mathcal{R}V + \frac{1}{2}\mathcal{R}\{\Gamma V\}V + O(\varepsilon^3),$$

where we have seen from Eq. (2.3) that $\mathcal{R}V$ is only a function of the actions in the nonresonant case. The assumption that $\boldsymbol{\omega}$ is nonresonant is a crucial hypothesis in Gallavotti's renormalization approach. Otherwise, a counterterm which only depends on the actions $\mathbf{A}$ cannot be found.

Our approach makes possible the construction of a control term in the resonant case. The controlled Hamiltonian is conjugate to $H_0+\mathcal{R}V$, where $\mathcal{R}V$ depends on the angle and action variables in the resonant case. Therefore the controlled Hamiltonian is not integrable in general. The new term $\mathcal{R}V$ which is always a conserved quantity is functionally independent of H_0 since it depends on the angles. There exists a linear canonical transformation $(\mathbf{A}', \boldsymbol{\varphi}') = ({}^t T \mathbf{A}, T^{-1}\boldsymbol{\varphi})$, where T is a $l \times l$ matrix with integer coefficients and determinant 1

such that $\boldsymbol{\omega}$ is mapped onto a new frequency vector which has its r last components equal to zero, where r denotes the dimension of $\{\mathbf{k} \in \mathbb{Z}^l$ such that $\boldsymbol{\omega}\cdot\mathbf{k}=0\}$. In these new coordinates $\mathcal{R}V$ depends only on r angles. This form of $H_0+\mathcal{R}V$ is called the *resonant normal form*. The nonresonant case occurs when $r=0$. When $r=1$ the normal form of $H_0+\mathcal{R}V$ depends only on one angle, so it is integrable.

In what follows, we will apply the control theory to a resonant Hamiltonian which models the $\mathbf{E} \times \mathbf{B}$ drift in magnetized plasmas.

III. CONTROL OF CHAOS IN A MODEL FOR $\mathbf{E} \times \mathbf{B}$ DRIFT IN MAGNETIZED PLASMAS

A. The model

In the guiding center approximation, the equations of motion of a charged particle in the presence of a strong toroidal magnetic field and of a time dependent electric field are [18]

$$\dot{\mathbf{x}} = \frac{d}{dt}\begin{pmatrix} x \\ y \end{pmatrix} = \frac{c}{B^2}\mathbf{E}(\mathbf{x},t) \times \mathbf{B} = \frac{c}{B}\begin{pmatrix} -\partial_y V(x,y,t) \\ \partial_x V(x,y,t) \end{pmatrix}, \tag{3.1}$$

where V is the electric potential, $\mathbf{E} = -\boldsymbol{\nabla}V$, and $\mathbf{B} = B\mathbf{e}_z$. The spatial coordinates x and y, where $(x,y) \in \mathbb{R}^2$ play the role of the canonically conjugate variables and the electric potential $V(x,y,t)$ is the Hamiltonian of the problem. To define a model we choose

$$V(\mathbf{x},t) = \sum_{\mathbf{k} \in \mathbb{Z}^2} V_{\mathbf{k}}\sin\left[\frac{2\pi}{L}\mathbf{k}\cdot\mathbf{x} + \varphi_{\mathbf{k}} - \omega(\mathbf{k})t\right], \tag{3.2}$$

where $\varphi_{\mathbf{k}}$ are random phases (uniformly distributed) and $V_{\mathbf{k}}$ decrease as a given function of $|\mathbf{k}|$, in agreement with experimental data [21]. In principle one should use for $\omega(\mathbf{k})$ the dispersion relation for electrostatic drift waves (which are thought to be responsible for the observed turbulence) with a frequency broadening for each $\mathbf{k}$ in order to model the experimentally observed spectrum $S(\mathbf{k},\omega)$. In order to use a simplified model we use in this paper $\omega(\mathbf{k}) = \omega_0$ constant as a dispersion relation. The phases $\varphi_{\mathbf{k}}$ are chosen at random in order to mimic a turbulent field with the reasonable hope that the properties of the realization thus obtained are not significantly different from their average. In addition we take for $|V_{\mathbf{k}}|$ a power law in $|\mathbf{k}|$ to reproduce the spatial spectral characteristics of the experimental $S(\mathbf{k})$, see Ref. [21]. Thus we consider the following explicit form of the electric potential:

$$V(x,y,t) = \frac{a}{2\pi} \sum_{\substack{m,n=1 \\ n^2+m^2 \leqslant N^2}}^{N} \frac{1}{(n^2+m^2)^{3/2}}$$

$$\times \sin\left[\frac{2\pi}{L}(nx+my) + \varphi_{nm} - \omega_0 t\right]. \tag{3.3}$$

By rescaling space and time, we can always assume that $L=1$ and $\omega_0=2\pi$. In what follows, we choose $N=25$. Figure 1 shows a visualization of the potential for $t=0$ and $a=1$. Since the model is fluctuating in time, the eddies of Fig. 1 are rapidly modified in time and where a vortex was ini-
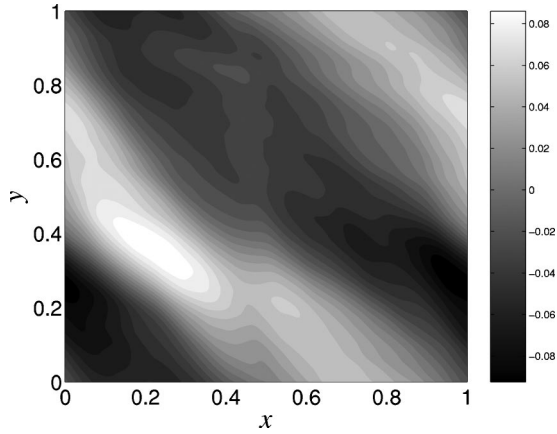
FIG. 1. Contour plot of $V(x,y,t)$ given by Eq. (3.3) for $t=0$, $a=1$, and $N=25$.

tially present, an open line appears, and so on.

Two particular properties of the model, anisotropy and propagation, have been observed: each image of the potential field shows an elongated structure of the eddies and superposing images obtained at different times a slight propagation in the $y=x$ direction is found. However, this propagation can easily be proved not to disturb the diffusive motion of the guiding centers. The property of propagation can be easily understood analytically. In fact, restricting ourselves to the most simplified case of an electric potential given only by a dominant mode ($n=m=1$) it is immediately evident that at any given time the maxima and minima of the sine are located on the lines $y=-x+$const. As the amplitudes are decreasing functions of n and m, this structure is essentially preserved also in the case of many waves. The property of anisotropy is an effect of the random phases in producing eddies that are irregular in space.

We notice that there are two typical time scales in the equations of motion: the drift characteristic time τ_d, inversely proportional to the parameter a, and the period of oscillation τ_ω of all the waves that enter the potential. The competition between these two time scales determines what kind of diffusive behavior is observed [11]. In what follows we consider the case of weak or intermediate chaotic dynamics (coexistence of ordered and chaotic trajectories) which corresponds to the quasilinear diffusion regime (see Sec. IV A), whereas in the case of fully developed chaos that corresponds to the so-called Bohm diffusion regime one has to introduce a slightly more complicated approach (see remark at the end of Sec. III C).

B. Computation of the control term

We extend the phase space (x,y) into (x,y,E,τ) where the new dynamical variable τ evolves as $\tau(t)=t+\tau(0)$ and E is its canonical conjugate. The autonomous Hamiltonian of the model is

$$H(x,y,E,\tau) = E + V(x,y,\tau). \quad (3.4)$$

The equations of motion are

$$\dot{x} = -\frac{\partial H}{\partial y} = -\frac{\partial V}{\partial y}, \quad \dot{y} = \frac{\partial H}{\partial x} = \frac{\partial V}{\partial x}, \quad \dot{\tau} = 1, \quad (3.5)$$

and E is given by taking H as constant along the trajectories. We absorb the constant c/B of Eq. (3.1) in the amplitude a of Eq. (3.3), so that we can assume that a is small when B is large. Thus, for small values of a, Hamiltonian (3.4) is in the form $H=H_0+\epsilon V$, which is an integrable Hamiltonian H_0 (with action-angle variables) plus a small perturbation ϵV. In our case $H_0=E$, i.e., independent of x,y, and τ, so that $\mathbf{A} = (E,x)$ and $\boldsymbol{\varphi}=(\tau,y)$ are action-angle coordinates for H_0 (y can be considered as an angle but it is frozen by the flow of H_0). We could have exchanged the role of x and y. We have

$$\boldsymbol{\omega}(\mathbf{A}) = \left(\frac{\partial H_0}{\partial E}, \frac{\partial H_0}{\partial x} \right) = (1,0),$$

that is, H_0 is resonant [i.e., $\boldsymbol{\omega}(\mathbf{A}) \cdot \mathbf{k}=0$ does not imply $\mathbf{k}=\mathbf{0}$]. In order to construct the operators Γ, $\mathcal{R}$, and $\mathcal{N}$ we consider

$$\frac{\partial}{\partial \boldsymbol{\varphi}} = \left(\frac{\partial}{\partial \tau}, \frac{\partial}{\partial y} \right),$$

so

$$\{H_0\} = \boldsymbol{\omega}(\mathbf{A}) \cdot \frac{\partial}{\partial \boldsymbol{\varphi}} = \frac{\partial}{\partial \tau}.$$

If we consider an element $W(x,y,\tau)$ of the algebra $\mathcal{A}$, periodic in time with period 1, we can write

$$W(x,y,\tau) = \sum_{k \in \mathbb{Z}} W_k(x,y)e^{2i\pi k\tau},$$

and the action of Γ, $\mathcal{R}$, and $\mathcal{N}$ operators on W is given by

$$\Gamma W = \sum_{k \neq 0} \frac{W_k(x,y)}{2ik\pi}e^{2i\pi k\tau},$$

$$\mathcal{R}W = W_0(x,y),$$

$$\mathcal{N}W = \sum_{k \neq 0} W_k(x,y)e^{2i\pi k\tau}. \quad (3.6)$$

If we apply the operator Γ to V given by Eq. (3.3), we obtain

$$\Gamma V = \frac{a}{(2\pi)^2} \sum_{\substack{n,m=1 \\ n^2+m^2 \leqslant N^2}} \frac{1}{(n^2 + m^2)^{3/2}}$$

$$\times \cos[2\pi(nx + my) + \varphi_{nm} - 2\pi\tau]. \quad (3.7)$$

Since V is periodic in time with zero mean value, we have $\mathcal{R}V=0$. In this case, as we have seen in the preceding section, Eqs. (2.8) and (2.9) give the expansion of the control term. If we add the exact expression of the control term to H_0+V, the effect on the flow is the confinement of the motion, i.e., the fluctuations of the trajectories of the particles, around their initial positions, are uniformly bounded for any time [20].
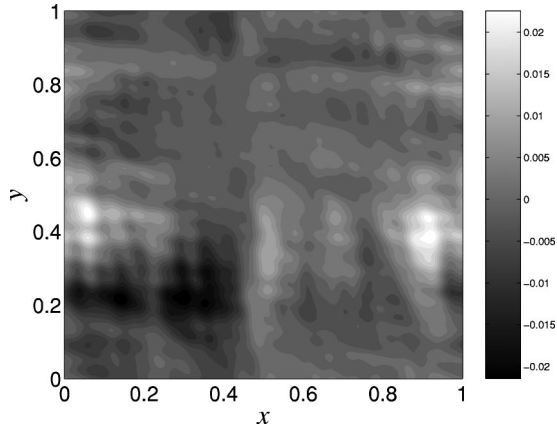
FIG. 2. Contour plot of f_2 given by Eq. (3.8) for $a=1$ and $N=25$.

FIG. 3. Contour plot of f_3 given by Eq. (3.9) for $t=0$, $a=1$, and $N=25$.

In the present paper we show that truncations of the exact control term f are able to regularize the dynamics and to slow down the diffusion. We compute the first terms of the series of the exact control terms f_2 and f_3. From Eq. (2.9) we have

$$f_2(V) = -\tfrac{1}{2}\{\Gamma V, V\},$$

and using the expressions of V and ΓV, we have

$$f_2(\mathbf{x}, \tau) = -\frac{a^2}{2(2\pi)^3} \sum_{\substack{n_1, m_1 \\ n_2, m_2}} \frac{1}{(n_1^2 + m_1^2)^{3/2}(n_2^2 + m_2^2)^{3/2}}$$

$$\times \{\cos[2\pi(n_1 x + m_1 y) + \varphi_{n_1 m_1} - 2\pi\tau],$$

$$\sin[2\pi(n_2 x + m_2 y) + \varphi_{n_2 m_2} - 2\pi\tau]\},$$

where $\{\cdot, \cdot\}$ is the Poisson bracket for x, y coordinates, i.e., for two generic functions f and g depending on x, y, τ, we have

$$\{f, g\} = \frac{\partial f}{\partial x}\frac{\partial g}{\partial y} - \frac{\partial f}{\partial y}\frac{\partial g}{\partial x}.$$

From Eqs. (3.3) and (3.7) we obtain

$$f_2(x, y, \tau) = \frac{a^2}{8\pi} \sum_{\substack{n_1, m_1 \\ n_2, m_2}} \frac{n_1 m_2 - n_2 m_1}{(n_1^2 + m_1^2)^{3/2}(n_2^2 + m_2^2)^{3/2}}$$

$$\times \sin\{2\pi[(n_1 - n_2)x + (m_1 - m_2)y]$$

$$+ \varphi_{n_1 m_1} - \varphi_{n_2 m_2}\}. \tag{3.8}$$

We notice that for the particular model (3.3) and for the particular choice of operator Γ given by Eq. (3.6), the partial control term f_2 is independent of time. Figure 2 depicts a contour plot of it.

The computation of f_3 is given by

$$f_3(V) = -\tfrac{1}{3}\{\Gamma V, f_2\},$$

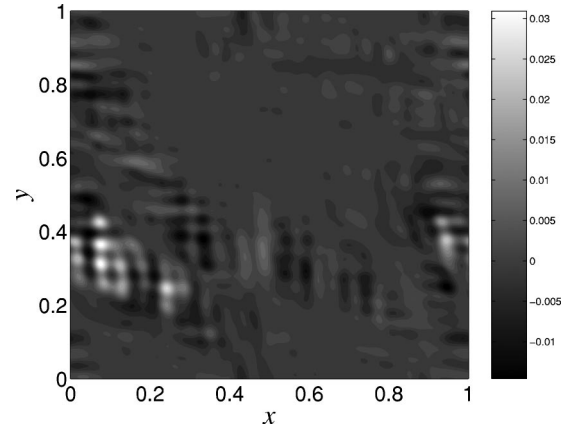and substituting the expressions (3.7) and (3.8) for ΓV and f_2, one obtains

$$f_3(x, y, \tau) = -\frac{a^3}{24\pi} \sum_{\substack{n_1, m_1, n_2, m_2 \\ n_3, m_3}}$$

$$\frac{(n_1 m_2 - m_1 n_2)[(n_1 - n_2)m_3 - (m_1 - m_2)n_3]}{(n_1^2 + m_1^2)^{3/2}(n_2^2 + m_2^2)^{3/2}(n_3^2 + m_3^2)^{3/2}}$$

$$\times \sin[2\pi(n_1 - n_2 + n_3)x + 2\pi(m_1 - m_2 + m_3)y$$

$$+ (\varphi_{n_1 m_1} - \varphi_{n_2 m_2} + \varphi_{n_3 m_3} - 2\pi\tau)]. \tag{3.9}$$

A contour plot of f_3 is depicted in Fig. 3. The computation of the other terms of the series (2.8) can be done recursively by using Eq. (2.9) (see also Ref. [20] and the Appendix).

C. Properties of the control term

In this section, we first state that for a sufficiently small, the exact control term exists and is regular. The proofs of these propositions are given in the Appendix. Then we give estimates of the partial control terms in order to compare the relative sizes of the different terms with respect to the perturbation.

Concerning the existence of the control term, we have the following proposition:

Proposition 3. If the amplitude a of the potential is sufficiently small, there exists a control term f given by the series (2.8) such that $E+V+f$ is canonically conjugate to E, where V is given by Eq. (3.3).

The proof is given in the Appendix. For $N=25$, it is shown that the control term exists for $a \lesssim 7 \times 10^{-3}$. As usual, such estimates are very conservative with respect to realistic values of a. In the numerical study, we consider values of a of order 1.

Concerning the regularity of the control term, we notice that each term f_s in the series (2.8) is a trigonometric polynomial with an increasing degree with s. The resulting control term is not smooth but its Fourier coefficients exhibit the same power law mode dependence as V.

Proposition 4. All the Fourier coefficients $f_{nmk}^{(s)}$ of the functions f_s of the series (2.8) satisfy

$$|f_{nmk}^{(s)}| \leq \frac{a^s C^s}{(n^2 + m^2)^{3/2}},$$

for $(n,m) \neq (0,0)$. Consequently, for sufficiently small values of a, the Fourier coefficients of the control term f given by Eq. (2.8) satisfy

$$|f_{nmk}| \leq \frac{C_\infty}{(n^2 + m^2)^{3/2}},$$

for $(n,m) \neq (0,0)$ and for some constant $C_\infty > 0$.

In order to measure the relative magnitude between Hamiltonian (3.3) and f_2 or f_3, we have numerically computed their mean squared values:

$$\sqrt{\frac{\langle f_2^2 \rangle}{\langle V^2 \rangle}} \approx 0.13a,$$

$$\sqrt{\frac{\langle f_3^2 \rangle}{\langle V^2 \rangle}} \approx 0.07a^2,$$

where $\langle f \rangle = \int_0^1 dt \int_0^1 dx \int_0^1 dy f(x,y,t)$.

Another measure of the relative sizes of the control terms is given by the electric energy density associated with each electric field V, f_2, and f_3. From the potential we get the electric field and hence the motion of the particles. We define an average energy density $\mathcal{E}$ as

$$\mathcal{E} = \frac{1}{8\pi} \langle |\mathbf{E}|^2 \rangle,$$

where $\mathbf{E}(x,y,t) = -\boldsymbol{\nabla} V$. In terms of the particles, it corresponds to the mean value of the kinetic energy $\langle \dot{x}^2 + \dot{y}^2 \rangle$ (up to a multiplicative constant). For $V(x,y,t)$ given by Eq. (3.3),

$$\mathcal{E} = \frac{a^2}{8\pi} \sum_{\substack{n,m=1 \\ n^2+m^2 \leq N^2}}^{N} \frac{1}{(n^2 + m^2)^2}. \tag{3.10}$$

We define the contribution of f_2 and f_3 to the energy density by

$$e_2 = \frac{1}{8\pi} \langle |\boldsymbol{\nabla} f_2|^2 \rangle, \tag{3.11}$$

$$e_3 = \frac{1}{8\pi} \langle |\boldsymbol{\nabla} f_3|^2 \rangle. \tag{3.12}$$

For $N=25$, these contributions satisfy

$$\frac{e_2}{\mathcal{E}} \approx 0.1a^2, \quad \frac{e_3}{\mathcal{E}} \approx 0.3a^4.$$

It means that the control terms f_2 and f_3 can be considered as small perturbative terms with respect to V when $a < 1$. We notice that even if f_3 has a smaller amplitude than f_2, its associated average energy density is larger for a of order 1 (more precisely for $a \gtrsim 0.58$).

Remark on the number of modes in V. In Sec. IV, all the computations have been performed for a fixed number of modes N ($N=25$) in the potential V given by Eq. (3.3). The question we address in this remark is how the results are modified as we increase N. First we notice that the potential and its electric energy density are bounded with N since

$$|V(x,y,t)| \leq a \sum_{n,m=1}^{\infty} \frac{1}{(n^2 + m^2)^{3/2}} < \infty,$$

$$\mathcal{E} \leq \frac{a^2}{8\pi} \sum_{n,m=1}^{\infty} \frac{1}{(n^2 + m^2)^2} < \infty.$$

Concerning the partial control term f_2, we see that it is in general unbounded with N. From its explicit form, one can see that it grows like $N \ln N$ (see the Appendix). Less is known about the control term since it is given by a series whose terms are defined by recursion. However, from the proof of Proposition 3 in the Appendix, we see that the value a of existence of the control term decreases like $1/(2N \ln N)$. This divergence of the control term comes from the fact that the Fourier coefficients of the potential V are weakly decreasing with the amplitude of the wave number.

Therefore, the exact control term might not exist if we increase N keeping a constant. However we will see in Sec. V B that for practical purposes the Fourier series of the control term can be truncated to its first terms (the Fourier modes with highest amplitudes). Furthermore in the example we consider as well as for any realistic situation the value of N is bounded by the resolution of the potential. In the case of electrostatic turbulence in plasmas $k\rho_i \sim 1$ determines an upper bound for k, where k is the transverse wave vector related to the indices n, m, and ρ_i the ion Larmor radius. The physics corresponds to the averaging effect introduced by the Larmor rotation.

Remark on the control in the Bohm regime (parameter a larger than 1). Let us define $V_0 \equiv V(t=0)$ and $\delta V = V - V_0$. Since the Bohm regime is defined as a regime of relatively slow evolution of the potential (with characteristic time τ_ω) compared to the motion of the particles (with characteristic time τ_d), $\tau_d < \tau_\omega$, one can introduce as small parameter $\epsilon \sim \tau_d / \tau_\omega$ and the integrable Hamiltonian $\bar{H}_0 = H_0 + V_0$, so that $H = \bar{H}_0 + \epsilon \tilde{V}$ with $\tilde{V} = (V - V_0)/\epsilon$. This approach is only valid for a finite time of order τ_ω after which one must redefine V_0, $\bar{H}_0$, and $\tilde{V}$.

IV. NUMERICAL INVESTIGATION OF THE CONTROL TERM

With the aid of numerical simulations (see Ref. [11] for more details on the numerics), we check the effectiveness of the control theory developed in Sec. III by comparing the dynamics of particles obtained from Hamiltonian (3.3) and from the same Hamiltonian with the control term f_2 given by Eq. (3.8), and with a more refined control term $f_2 + f_3$, where f_3 is given by Eq. (3.9). We use three types of indicators of the dynamics: diffusion coefficient, Lyapunov indicators, and probability distribution function (PDF) of step sizes.
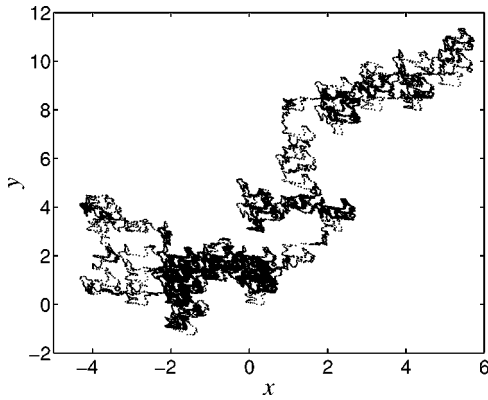
FIG. 4. Poincaré surface of section of a trajectory obtained for Hamiltonian (3.3) using a generic initial condition assuming $a=0.8$.

A. Diffusion of test particles

The effect of the control terms can first be seen from a few randomly chosen trajectories. We have plotted Poincaré sections (which are stroboscopic plots with period 1 of the trajectories of V). In Figs. 4 and 5 is plotted the Poincaré surfaces of section of two trajectories issued from generic initial conditions computed without and with the control term f_2, respectively. Similar pictures are obtained for many other randomly chosen initial conditions. The stabilizing effect of the control term (3.8) is illustrated by such trajectories. The motion remains diffusive but the extension of the phase space explored by the trajectory is reduced.

In order to study the diffusion properties of the system, we have considered a set of $\mathcal{M}$ particles (of order 1000) uniformly distributed at random in the domain $0 \leqslant x, y \leqslant 1$ at $t=0$. We have computed the mean square displacement $\langle r^2(t) \rangle$ as a function of time,

$$\langle r^2(t) \rangle = \frac{1}{\mathcal{M}} \sum_{i=1}^{M} |\mathbf{x}_i(t) - \mathbf{x}_i(0)|^2, \qquad (4.1)$$

where $\mathbf{x}_i(t) = (x_i(t), y_i(t))$ is the position of the ith particle at time t obtained by integrating Eq. (3.5) with initial condition
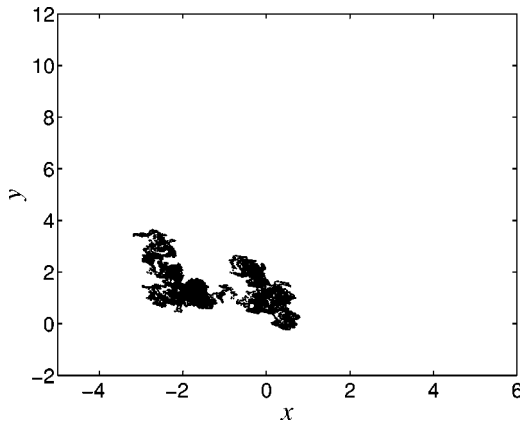
FIG. 5. Poincaré surface of section of a trajectory obtained using a generic initial condition as in Fig. 1 and adding the control term (3.8) to Hamiltonian (3.3) with $a=0.8$.
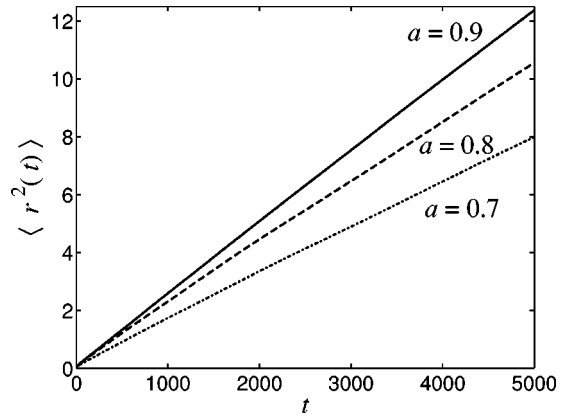

FIG. 6. Mean square displacement $\langle r^2(t) \rangle$ vs time t obtained for Hamiltonian (3.3) with three different values of $a=0.7, 0.8, 0.9$.

$\mathbf{x}_i(0)$. In Fig. 6 is presented $\langle r^2(t) \rangle$ for three different values of a: $a=0.7$, $a=0.8$, and $a=0.9$. For the range of parameters we consider the behavior of $\langle r^2(t) \rangle$ is always found to be linear in time for t large enough. The corresponding diffusion coefficient is defined as

$$D = \lim_{t \to \infty} \frac{\langle r^2(t) \rangle}{t}.$$

The values of D as a function of a with and without control term are presented in Fig. 7. A significant decrease of the diffusion coefficient when the control term f_2 is added can be readily observed. As expected, the action of the control term gets weaker as a is increased towards the strongly chaotic region.

B. Lyapunov indicator method

In order to get insight into the action of the control term to the dynamics, we apply the Lyapunov indicator method. This method provides local information in phase space. It has been introduced to detect ordered and chaotic trajectories in the set of initial conditions. It associates a finite-time Lyapunov exponent ν with an initial condition $\mathbf{x}_0$. By look-
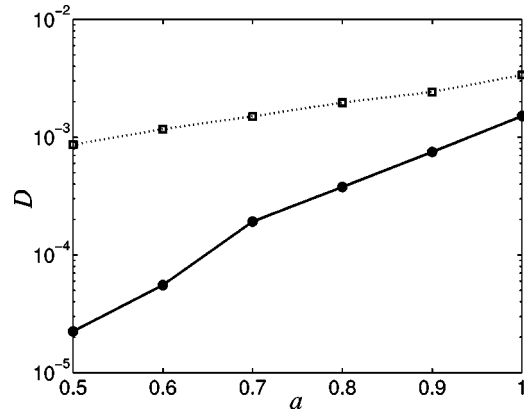

FIG. 7. Diffusion coefficient D vs a obtained for Hamiltonian (3.3) (open squares) and Hamiltonian (3.3) plus control term (3.8) (full circles).

ing at the map $\mathbf{x}_0 \mapsto \nu(\mathbf{x}_0)$, one distinguishes the set of initial conditions leading to regular motion associated with a small finite-time Lyapunov exponent. The pictures of this map show the phase space structures where the motion is trapped and does not diffuse throughout the phase space, e.g., they highlight islands of stability located around elliptic periodic orbits.

Consider an autonomous flow $\dot{\mathbf{x}} = f(\mathbf{x})$. The Lyapunov indicator method is based on the analysis of the tangent flow

$$\frac{d\mathbf{y}}{dt} = Df(\mathbf{x})\mathbf{y}, \qquad (4.2)$$

where Df is the matrix of variations of the flow. The Lyapunov indicator is defined as the value

$$\nu(\mathbf{x}_0, T) = \ln\|\mathbf{y}(T)\|,$$

at some finite time T starting with some initial condition $\mathbf{x}_0$ and a generic vector $\mathbf{y}_0$. This definition is very close to the one of a finite-time Lyapunov exponent. The plot of ν versus $\mathbf{x}_0$ gives a map of the dynamics by highlighting regions of stability and regions of chaotic dynamics.

For a chaotic trajectory, the value of the Lyapunov indicator increases linearly with time, whereas for a regular trajectory (periodic or quasiperiodic), it increases like $\ln t$ (see rigorous results for nearly perturbed Hamiltonian systems in Ref. [22]). So in regular regions, this Lyapunov indicator is expected to be much lower than in chaotic regions.

Here the Hamiltonian flow is not autonomous. However, by considering that t is a new coordinate of the motion (and E is its conjugate momentum), we obtain an autonomous flow with two degrees of freedom. We notice that the equations of motion for Hamiltonian (3.3) can be written as

$$\dot{\mathbf{x}} = \mathrm{Re}[\mathbf{F}(\mathbf{x})e^{-2i\pi t}], \qquad (4.3)$$

where

$$\mathbf{F}(\mathbf{x}) = \nabla^\perp V(\mathbf{x}, 0) + i\nabla^\perp V(\mathbf{x}, 1/4),$$

where $\nabla^\perp = (-\partial/\partial y, \partial/\partial x)$ and $V(\mathbf{x}, t)$ is given by Eq. (3.3). The nonautonomous flow (4.3) can be mapped into an autonomous flow by considering a third equation $\dot{\tau} = 1$. The computation of the tangent flow (of dimension 3) follows from the matrix of variations of the autonomous flow. We have chosen the third component of the vector $\mathbf{y}$ following the evolution of the tangent flow (4.2) equal to one, which can be done without loss of generality since Eq. (4.2) is linear in $\mathbf{y}$. Therefore, it reduces to the evolution of a two-dimensional vector $\mathbf{y}$ which is given by

$$\dot{\mathbf{y}} = \mathrm{Re}[G(\mathbf{x})e^{-2i\pi t}]\mathbf{y} + 2\pi\mathrm{Im}[\mathbf{F}(\mathbf{x})e^{-2i\pi t}],$$

where G is the two-dimensional matrix $G(\mathbf{x}) = D\mathbf{F}$ (matrix of the variations of the vector field $\mathbf{F}$). Figure 8 shows the value of $\nu(\mathbf{x}_0, T)$ as a function of T for $T \in [0, 140]$ for three initial conditions $\mathbf{x}_0$: one strongly chaotic $\mathbf{x}_0 = (0.865, 0.39)$, one weakly chaotic $\mathbf{x}_0 = (0.8766, 0.39)$, and one quasiperiodic $\mathbf{x}_0 = (0.895, 0.39)$. The plots of the Poincaré sections of these three trajectories up to $T = 1000$ are shown in Fig. 9. These figures show two chaotic trajectories for which
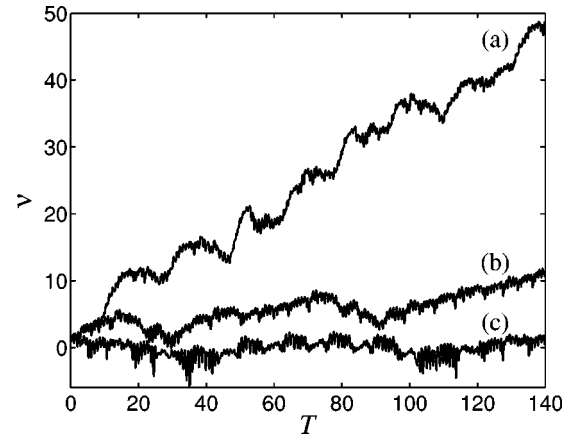

FIG. 8. Values of the Lyapunov indicator $\nu(\mathbf{x}_0, T)$ as a function of time T for three trajectories obtained for Hamiltonian (3.3) with $a = 0.4$ for the following initial conditions: one strongly chaotic (a) $\mathbf{x}_0 = (0.865, 0.39)$, one weakly chaotic (b) $\mathbf{x}_0 = (0.8766, 0.39)$, and one quasiperiodic (c) $\mathbf{x}_0 = (0.895, 0.39)$.

there is an overall linear increase of the Lyapunov indicator, and one quasiperiodic motion (trapped around an elliptic periodic orbit). We notice that not only the method is able to discriminate early between regular and chaotic motions but it is also able to detect weakly versus strongly chaotic trajectories for rather small values of T.

With the control term f_2 given by Eq. (3.8), the equations of motion can be rewritten as

$$\dot{\mathbf{x}} = \mathrm{Re}[\mathbf{F}e^{-2i\pi t}] + \mathbf{f}_2(\mathbf{x}),$$

where $\mathbf{f}_2(\mathbf{x}) = \nabla^\perp f_2$. The equation of evolution of $\mathbf{y}$ becomes

$$\dot{\mathbf{y}} = \mathrm{Re}[G(\mathbf{x})e^{-2i\pi t}]\mathbf{y} + 2\pi\mathrm{Im}[\mathbf{F}(\mathbf{x})e^{-2i\pi t}] + Df_2(\mathbf{x})\mathbf{y}.$$

With the control term $f_2(\mathbf{x}) + f_3(\mathbf{x}, t)$, where f_3 is given by Eq. (3.9), the equations of motion can be written as

$$\dot{\mathbf{x}} = \mathrm{Re}[(\mathbf{F} + \mathbf{f}_3)e^{-2i\pi t}] + \mathbf{f}_2(\mathbf{x}),$$

where $\mathbf{f}_3(\mathbf{x}) = \nabla^\perp f_3(\mathbf{x}, 0) + i\nabla^\perp f_3(\mathbf{x}, 1/4)$. The equation of evolution of $\mathbf{y}$ becomes
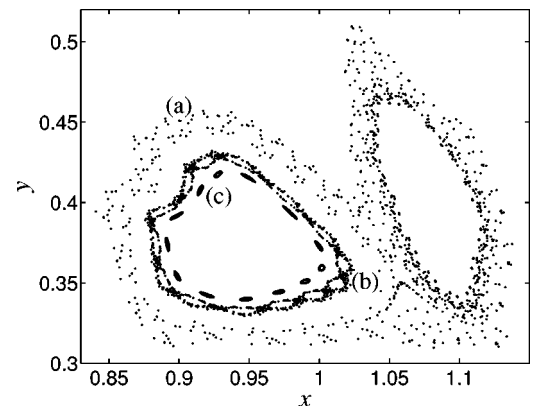

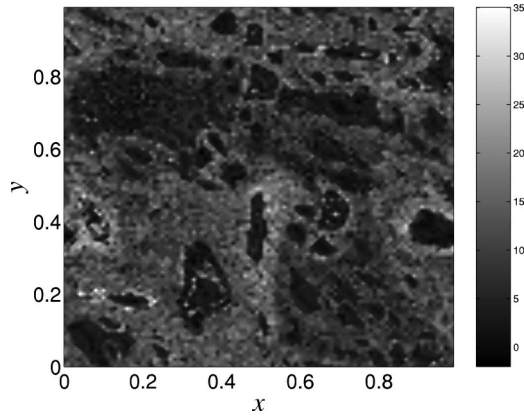FIG. 9. Poincaré sections of the three trajectories of Fig. 8.

FIG. 10. Lyapunov indicator map $\nu(\mathbf{x}_0, T=200)$ for Hamiltonian (3.3) for $a=0.4$.

$$\dot{\mathbf{y}} = \mathrm{Re}[(G + g_3)e^{-2i\pi t}]\mathbf{y} + 2\pi\mathrm{Im}[(\mathbf{F} + \mathbf{f}_3)e^{-2i\pi t}] + D f_2 \mathbf{y},$$

where $g_3(\mathbf{x}) = D\mathbf{f}_3$.

On a grid of 10 000 initial conditions $\mathbf{x}_0 \in [0,1]^2$, we compute $\nu(\mathbf{x}_0, T)$ for $T=200$. Figure 10 represents the Lyapunov indicator map for $a=0.4$ without control term. Figure 11 shows for the same values of parameters, the Lyapunov indicator map with the control term f_2. The general effect of the control term f_2 is a decrease of the magnitude of the Lyapunov indicators. However, the stabilization effect of the control term f_2 is not uniform. There are regions where the (partial) control term f_2 fails to stabilize the trajectories, e.g., in the region near $\mathbf{x}_0 = (0.1, 0.4)$. Figure 12 plots the Poincaré section of the trajectories starting at $\mathbf{x}_0 = (0.085, 0.385)$ for Hamiltonian (3.3) with and without the control term f_2 given by Eq. (3.8). We notice that this trajectory is more chaotic and more diffusive with the control term than without.

In order to see the global stabilization effect of the partial control term f_2, we notice from the values plotted in Fig. 10 that for $a=0.4$ about 25% of the trajectories have a Lyapunov indicator less than 5 at $T=200$ without the control term f_2, compared with 70% with the control term (from Fig. 11). Figure 13 represents the histograms of the Lyapunov indica-
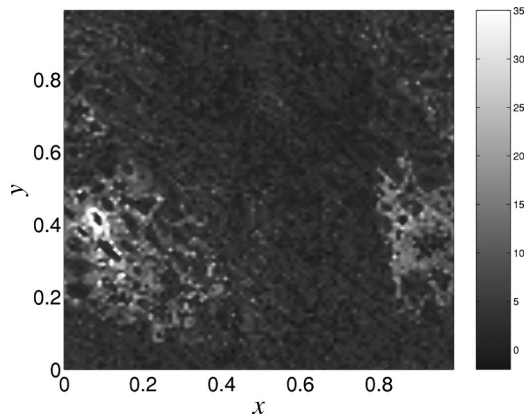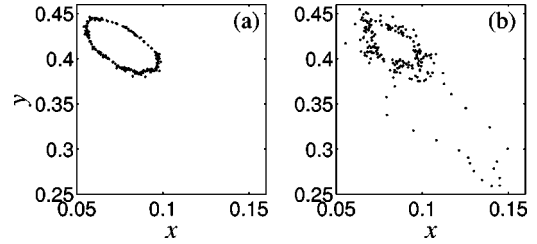

FIG. 12. Poincaré sections of the trajectories of (a) Hamiltonian (3.3) and (b) Hamiltonian (3.3) with control term f_2 given by Eq. (3.8), with initial conditions $\mathbf{x}_0 = (0.085, 0.385)$.

tor at $T=200$ for $a=0.4$ with and without control term. The first peak in the upper and lower panels corresponds to the regular component of the phase space. We clearly see that the second peak corresponding to the chaotic component is drastically reduced with the addition of the partial control term. The effect of a more refined control term is observed in Fig. 14 for $a=0.6$ when the control term f_2 starts to fail to reduce significantly the chaotic part of phase space. We see that the proportion of the regular trajectories has increased with the addition of f_3. More quantitatively, 8% of the trajectories of the Hamiltonian without control have a Lyapunov indicator smaller than 7 at $T=200$. With the addition of f_2, this proportion is increased to 25% whereas it is around 30% with the addition of f_3.

C. Horizontal step sizes

In order to investigate the effect of the control term on the transport properties and its relationship with single trajectories, we have computed the PDF of the step sizes. Let us define the *horizontal step size* (vertical step size) as the distance covered by the test particle between two successive sign reversals of the horizontal (vertical) component of the drift velocity. The effect of the control is analyzed in terms of the PDF of step sizes. Following test particle trajectories for a large number of initial conditions, with and without control, leads to the PDFs plotted in Fig. 15 for Hamiltonian (3.3) without and with control term (3.8) for $a=0.7$. A marked reduction of the PDF is observed at large step sizes

FIG. 11. Lyapunov indicator map $\nu(\mathbf{x}_0, T=200)$ for Hamiltonian (3.3) for $a=0.4$ with the control term f_2 given by Eq. (3.8).
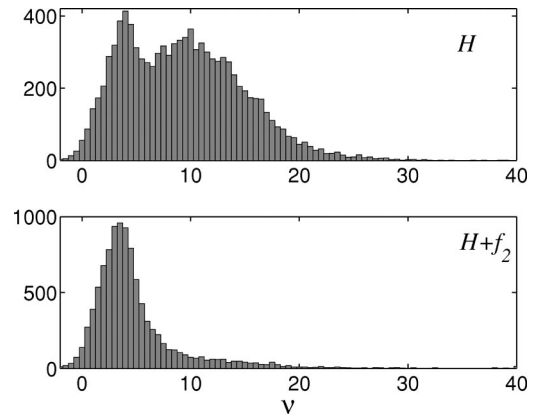

FIG. 13. Histograms of the Lyapunov indicators at $T=200$ for $a=0.4$ with and without control term computed in Figs. 10 and 11.
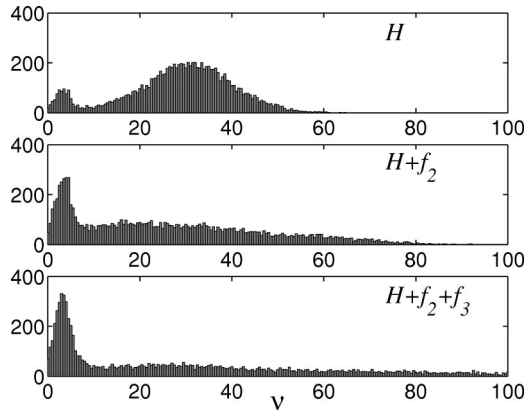
FIG. 14. Histograms of the Lyapunov indicators at $T=200$ for $a=0.6$ without control term (upper panel), with control term f_2 (middle panel), and with control term f_2+f_3 (lower panel).

with control relatively to the uncontrolled case. Conversely, an increase is found for the smaller step sizes. The control quenches the large steps (typically larger than 0.5 for $a=0.7$). Such a reduction of the probability to achieve a large radial step will modify the transport efficiency and, in particular, reduce the diffusion coefficient.

In order to give support that the first peak of the histogram of the Lyapunov indicator (see Fig. 13) is associated with the small step sizes, we have plotted in Fig. 16 the distribution of horizontal step sizes of the trajectories with a small Lyapunov indicator (smaller than 7), and also the same PDF for trajectories associated with large Lyapunov indicator (larger than 7). This result gives support to the fact that the control term reduces the diffusion of trajectories by reducing chaos in the system (by the creation of invariant tori [23], see also the global picture in the conclusion).

V. ROBUSTNESS OF THE CONTROL

In the preceding section, we have seen that a truncation of the series defining the control term by considering the first or

FIG. 16. PDF of the horizontal step sizes of the trajectories with small Lyapunov indicator (smaller than 7, full squares) and with large Lyapunov indicator (larger than 7, open squares) for Hamiltonian (3.3) with $a=0.4$.

the two first terms in the perturbation series in ϵ gives a very efficient control on the chaotic dynamics of the system.

In this section we show that it is possible to use an approximate control or to make a small error while computing the control term and still get an efficient control of the dynamics.

Below, we give numerical evidence for the following statements: the reduction of the amplitude shows that one can inject less energy to achieve a significant control. The truncation of the Fourier series indicates that one can simplify the control term and still get a significant control. The change of phases shows that one can introduce some error in the phases and still get a significant control.

A. Reduction of the amplitude of the control term

We check the robustness of the control by increasing or reducing the amplitude of the control [24]. We replace f_2 by δf_2 and we vary the parameter δ away from its reference
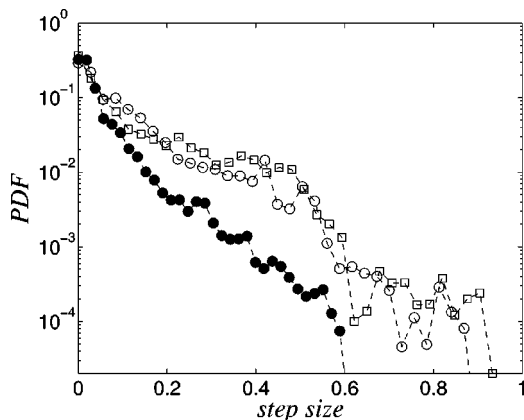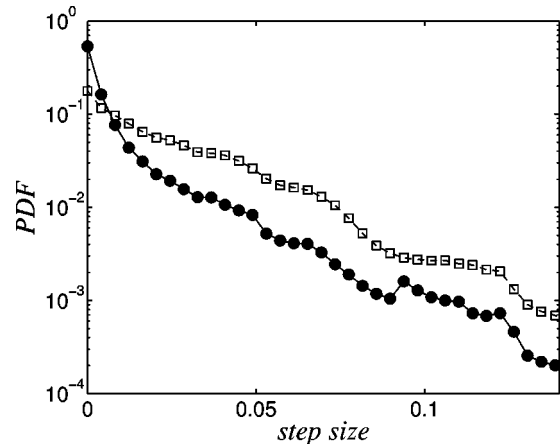

FIG. 15. PDF of the magnitude of the horizontal step size for Hamiltonian (3.3) with $a=0.7$ without the control term (open squares), with the control term f_2 (full circles), and with a truncated control term with 12 modes (open circles).
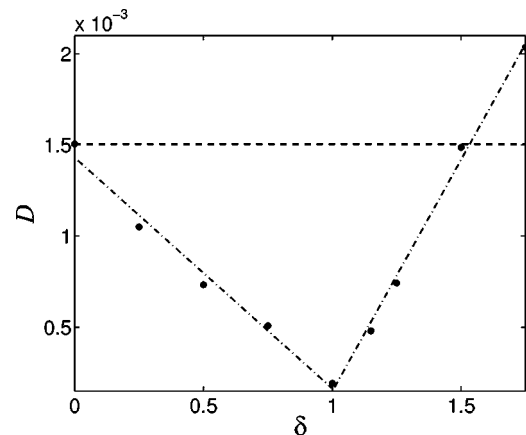

FIG. 17. Diffusion coefficient D vs the magnitude of the control term (3.8) for $a=0.7$. The horizontal dashed line corresponds to the value of D without control term. The dash-dotted line is a piecewise linear interpolation.
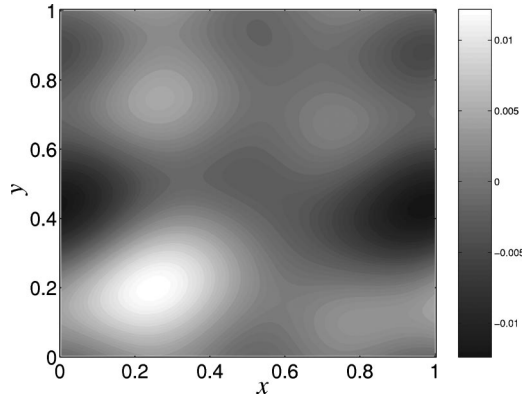
FIG. 18. Contour plot of the truncation of $f_2(x,y)$ for $a=0.7$ containing the 12 Fourier modes of highest amplitude.

value $\delta=1$. Figure 17 shows that both the increase and the reduction of the magnitude of the control term (which is proportional to δa^2) result in a loss of efficiency in reducing the diffusion coefficient. The fact that a larger perturbation term—with respect to the computed one—does not work better also means that the control is "smart" and that it is not a "brute force" effect.

The interesting result is that one can significantly reduce the amplitude of the control ($\delta<1$) and still get a reduction of the chaotic diffusion. We notice that the average energy density $e_2(\delta)$ associated with a control term δf_2 is equal to $e_2(\delta)=\delta^2 e_2$, where e_2 is given by Eq. (3.11). Therefore, for $\delta=0.5$, where the energy necessary for the control is one-fourth of the optimal control, the diffusion coefficient is significantly smaller than in the uncontrolled case (nearly factor 3).

B. Truncation of the Fourier series of the control term

We show that a reduction of the number of Fourier modes of f_2 can still significantly reduce chaotic diffusion. The Fourier expansion of the control term f_2 given by Eq. (3.8) is

$$f_2 = \sum_{n,m} f_{nm}^{(2)} e^{2i\pi(nx+my)}, \qquad (5.1)$$

where $f_{nm}^{(2)}$ is

$$f_{nm}^{(2)} = \frac{a^2}{8\pi i} \sum_{n_1,m_1} \frac{(nm_1 - n_1 m) e^{i(\varphi_{n_1 m_1} - \varphi_{n_1-n, m_1-m})}}{(n_1^2 + m_1^2)^{3/2}[(n_1-n)^2 + (m_1-m)^2]^{3/2}}. \qquad (5.2)$$

The truncation of the Fourier series is made by considering the Fourier modes with an amplitude greater than or equal to ϵ, that is, the sum in Eq. (5.2) is restricted to the set of modes (n,m) such that $|f_{nm}^{(2)}| \geq \epsilon$. For example, if we consider $\epsilon \simeq 9 \times 10^{-4}$, there are 12 modes in the sum, which are the modes with wave vector $(0,1)$, $(0,2)$, $(1,-1)$, $(1,-2)$, $(1,0)$, $(2,0)$ and the opposite wave vectors (f_2 is real), compared with the total number of modes of the full f_2 which is about 2000. Figure 18 shows the contour plot of f_2 obtained with only these 12 modes. Figure 19 shows the diffusion coefficient for the dynamics of the truncated
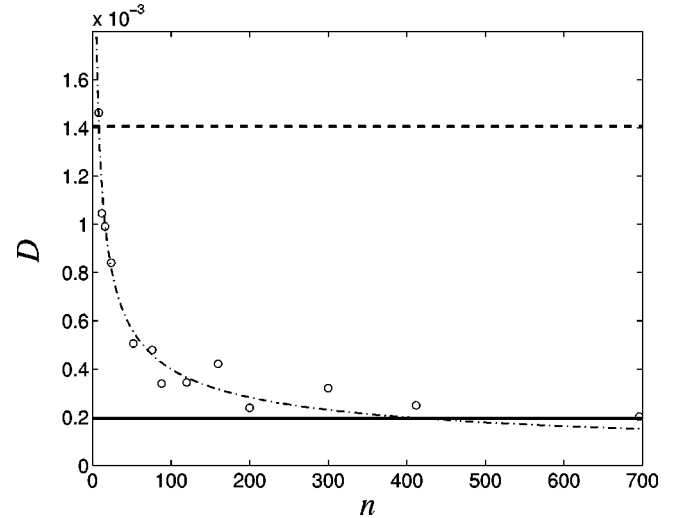

FIG. 19. Diffusion coefficient D vs the number of Fourier modes n in the truncation of the control term f_2 for $a=0.7$. The dashed line corresponds to the case without control term, the solid line corresponds to the value of the diffusion with the full control term f_2, and the dash-dotted line corresponds to a power law interpolation ($\propto n^{-1/2}$).

control term versus the number of Fourier modes kept in the truncation of f_2. The reduction of the diffusion (with respect to the uncontrolled case) also holds for a very simplified control term containing only the few highest Fourier modes of the full control term. If we replace f_2 by the truncation with 12 modes we see that the effect is still a strong reduction of the diffusion coefficient, a reduction of about 25%. The energy density $e_2^{(12)}$ (see Sec. III C) of this truncated control term with respect to the energy density $\mathcal{E}$ is

$$\frac{e_2^{(12)}}{\mathcal{E}} \simeq 0.009 a^2, \qquad (5.3)$$

where $\mathcal{E}$ is given by Eq. (3.10), which is less than 1% of the energy associated to the electric potential. It is interesting to note that the energy density of this truncation with respect to the one of the full control term f_2 is

$$\frac{e_2^{(12)}}{e_2} \simeq 0.09, \qquad (5.4)$$

where e_2 is given by Eq. (3.11), which is less than 10% of the energy associated with the full control term f_2. Moreover, we see from Fig. 15, where the PDF of horizontal step sizes is plotted, that the effect of this coarse grained control term f_2 reduced to 12 modes is also to quench large step sizes.

More generally, these results show that a partial knowledge of the potential, e.g., on a grid (coarse grained), is sufficient to obtain a significant control of the dynamics.

C. Change of phases in f_2

We check the robustness of the control with respect to an error introduced in the phases of the control term given by
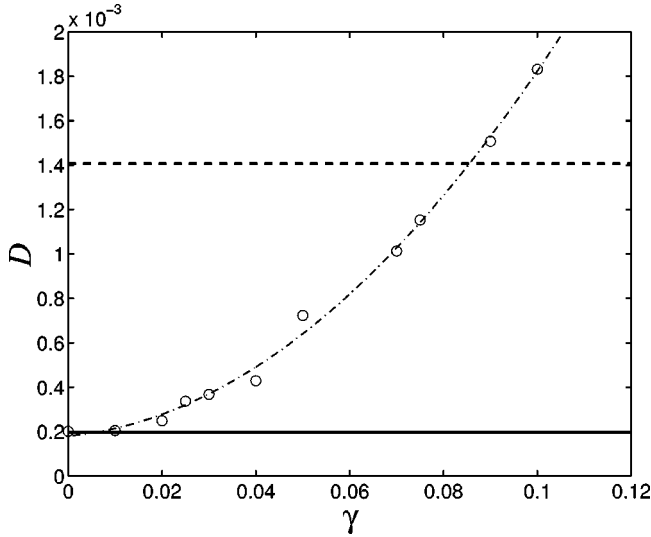
FIG. 20. Diffusion coefficient D vs the phase error γ in the expression (3.8) of f_2 for $a=0.7$. The dashed line corresponds to the case without control term, the solid line corresponds to the case with the full control term, and the dash-dotted line corresponds to a quadratic interpolation.

Eq. (3.8), i.e., we change the phases φ_{nm} by $\widetilde{\varphi}_{nm}$ in Eq. (3.8) by

$$\widetilde{\varphi}_{nm} = \varphi_{nm} + \gamma\varphi_{nm}^{err}, \qquad (5.5)$$

where φ_{nm}^{err} are uniformly random distributed phases in $[0,2\pi]$, γ is the amplitude of the error, and φ_{nm} are the correct phases. Figure 20 shows the diffusion coefficient versus the phase error γ for a fixed value of $a(a=0.7)$. We notice that the chaotic diffusion is still significantly reduced by the control with a small error on the phases. The diffusion coefficient is still strongly reduced by a factor greater than 2 for a phase error of 5%. For small values of γ the diffusion coefficient versus γ is well fitted by a quadratic interpolation, that is, $D(\gamma)=D_0+D_1\gamma^2$.

VI. CONCLUSIONS

We have provided an effective strategy to control the chaotic diffusion in Hamiltonian dynamics using small perturbations. Since the formula of the control term is explicit, we are able to compare the dynamics without and with control. The idea of the control is pictorially represented in Fig. 21: A Hamiltonian $H_0+\varepsilon V$ is controlled by adding a control term f. The naive choice for a control term would be $f=-\varepsilon V$ but this would be useless since it is of the same magnitude of the source of chaotic transport and thus would require a major modification of the physical condition of the system of interest. In this paper, we have presented a way to design an integrable controlled Hamiltonian H_c with a *small* control term f of order ε^2. This controlled Hamiltonian is conjugate to H_0 (we assume for simplicity that $\mathcal{R}V=0$). This construction of the controlled Hamiltonian works well up to some value ε_1. Moreover, we have shown that the control is robust, in the sense that one can use an approximate controlled
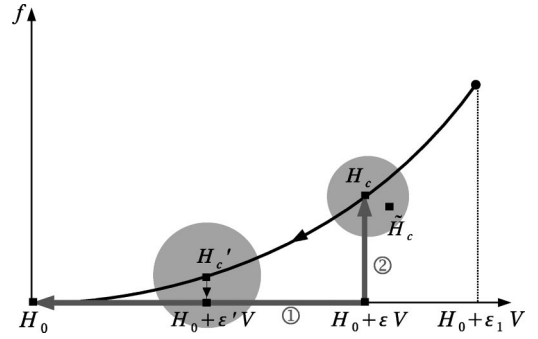

FIG. 21. Global picture of the control: The bold curved segment of curve represents a set of integrable Hamiltonians around H_0. The gray circles are the domains of existence of a given invariant torus around an integrable Hamiltonian. The gray arrows represent two ways of controlling the Hamiltonian $H_0+\varepsilon V$: the first one of order ε and the second one of order ε^2. The arrows from H_c to H_c' and from H_c' to $H_0+\varepsilon'V$ represent close to identity canonical transformations.

Hamiltonian $\widetilde{H}_c$ which is not integrable but—being sufficiently close to H_c—generates a more regular dynamics (presence of invariant tori) with respect to $H_0+\varepsilon V$. For instance, we have shown that one can successfully use a truncated control term of order ϵ^2 and that one is allowed to tailor it to some specific requirements on its shape, on the energy necessary to achieve control, and also according to a partial knowledge of V (e.g., a truncation of the Fourier series and an error on the phases).

The invariant tori that have been created by adding the control term f of order ε^2 are those which were broken by increasing the amplitude of the perturbation, meaning that these tori are those of a Hamiltonian $H_0+\varepsilon'V$, where $\varepsilon'<\varepsilon$ (up to some smooth canonical transform close to the identity transform). In order to illustrate this statement, we have plotted in gray two regions of existence of a given invariant torus (specified, e.g., by its frequency). The uncontrolled Hamiltonian $H_0+\varepsilon V$ does not have this invariant torus whereas the controlled one $H_c=H_0+\varepsilon V+\varepsilon^2 f$ does. The controlled Hamiltonian H_c is conjugate to the controlled Hamiltonian $H_c' =H_0+\varepsilon'V+\varepsilon'^2f$ for $\varepsilon'<\varepsilon$ (since they are both conjugate to H_0). Since $H_0+\varepsilon'V$ is inside the ball around the integrable Hamiltonian H_c', the invariant torus of $H_0+\varepsilon'V$ of the selected frequency is a small deformation of the torus of the controlled Hamiltonian H_c' and hence a small deformation of the torus of the controlled Hamiltonian H_c. Therefore the invariant tori of H_c obtained by means-of control are small deformations of the tori of $H_0+\varepsilon V$ which were broken by increasing ε.

We have applied this general technique of control to a specific model, describing anomalous electric transport in magnetized plasmas. In particular, we have shown that the control term is robust, meaning that one is able to simplify it, to reduce its amplitude or to make a small error without changing its overall action of reducing chaotic transport. Even though we use a rather simplified model to describe chaotic transport of charged particles in fusion plasmas, our result makes us believe that through some small smart modification of the electric potential a relevant reduction of the

turbulent losses of energy and particles in tokamaks could be attained, for the moment at least in principle.

APPENDIX: PROOF OF PROPOSITIONS 3 AND 4

1. Proof of Proposition 3

The terms of the series (2.8) can be written in the following form:

$$f_s = \sum_{n,m,k} f_{nmk}^{(s)} \sin[2\pi(nx+my)+\varphi_{nmk}^{(s)}-2\pi kt],$$

where the sum over k is from $-s$ to s, and the two sums over n and m are from $-sN$ to sN. From the recursion formula (2.9), we have

$$f_{n'm'k'}^{(s)} = \frac{a}{2s} \sum_{n,m=1}^{N} \frac{mn'-nm'}{(n^2+m^2)^{3/2}} \times (-f_{n'-n,m'-m,k'-1}^{(s-1)} + f_{n-n',m-m',k'+1}^{(s-1)}). \tag{A1}$$

We use the following norm:

$$\|f_s\| = \sup_{n,m,k} |f_{nmk}^{(s)}|.$$

From Eq. (A1), we get

$$\|f_s\| \leq \frac{a\|f_{s-1}\|}{s} \sup_{n',m'} \sum_{n,m=1}^{N} \frac{|mn'-nm'|}{(n^2+m^2)^{3/2}}.$$

Since, $|mn'-nm'| \leq sN(m+n)$, we have

$$\|f_s\| \leq a\lambda \|f_{s-1}\|,$$

where

$$\lambda = 2N \sum_{n,m=1}^{N} \frac{m}{(n^2+m^2)^{3/2}}. \tag{A2}$$

It follows that

$$\|f_s\| \leq (a\lambda)^{s-1} a 2^{-3/2},$$

since $\|f_1\| = a2^{-3/2}$. Therefore, the series (2.8) converges for $a < 1/\lambda$. We notice that for $N=25$, $\lambda \approx 135$, i.e., the series converges for $a \lesssim 7 \times 10^{-3}$.

Since $n \mapsto m/(n^2+m^2)^{3/2}$ is a positive and decreasing function, we have

$$\sum_{n=1}^{N} \frac{m}{(n^2+m^2)^{3/2}} \leq \int_0^N \frac{m\,dn}{(n^2+m^2)^{3/2}} \leq \int_0^\infty \frac{m\,dn}{(n^2+m^2)^{3/2}}.$$

By rescaling the integral ($t=n/m$) and using the fact that $\int_0^\infty dt/(t^2+1)^{3/2}=1$, we have

$$\lambda \leq 2N \sum_{m=1}^{N} \frac{1}{m} \leq 2N \ln N + 2\gamma N + 1, \tag{A3}$$

where γ is the Euler-Mascheroni constant. In particular, we notice that the bound on λ increases like $N \ln N$.

2. Proof of Proposition 4

Concerning the regularity of the functions f_s and f, we would like to show that

$$|f_{nmk}^{(s)}| \leq \frac{a^s C^s}{(n^2+m^2)^{3/2}}. \tag{A4}$$

We notice that Eq. (A4) is satisfied for $f_1=V$ given by Eq. (3.3) for $C \geq 1$. The inequality (A1) gives

$$|f_{n'm'k'}^{(s)}| \leq a^s \frac{C^{s-1}}{s}$$

$$\times \sum_{n,m=1}^{N} \frac{|mn'-nm'|}{(n^2+m^2)^{3/2}[(n'-n)^2+(m'-m)^2]^{3/2}}.$$

We can always assume that both n' and m' are positive since we have $|n'-n| \geq ||n'|-n|$ which gives

$$|f_{n'm'k'}^{(s)}| \leq Na^s C^{s-1}$$

$$\times \sum_{n,m=1}^{N} \frac{m+n}{(n^2+m^2)^{3/2}[(|n'|-n)^2+(|m'|-m)^2]^{3/2}},$$

where we have used the inequality $|mn'-nm'| \leq sN(m+n)$.

We have to distinguish the following cases: (i) $n' > N$ and $m' > N$, (ii) $n' \leq N$ and $m' > N$, and (iii) $n' \leq N$ and $m' \leq N$. We notice that by symmetry the case $n' > N$ and $m' \leq N$ is similar to (ii).

For $n',m' > N$, we have $n' \leq (N+1)(n'-n)$ and $m' \leq (N+1)(m'-m)$. Thus we have

$$\frac{1}{(n'-n)^2+(m'-m)^2} \leq \frac{(N+1)^2}{n'^2+m'^2},$$

which leads to

$$|f_{n'm'k'}^{(s)}| \leq \frac{a^s C^{s-1}(N+1)^3 \lambda}{(n'^2+m'^2)^{3/2}},$$

where λ is given by Eq. (A2).

For $n' \leq N$ and $m' > N$, we have $m' \leq (N+1)(m'-m)$. By using the estimate $(n'-n)^2+(m'-m)^2 \geq (m'-m)^2$, we have

$$\frac{1}{(n'-n)^2+(m'-m)^2} \leq \frac{(N+1)^2}{m'^2},$$

and since $n' \leq m'$,

$$\frac{(N+1)^2}{m'^2} \leq \frac{2(N+1)^2}{n'^2 + m'^2}.$$

Thus we have

$$|f_{n'm'k'}^{(s)}| \leq \frac{a^s C^{s-1} 2^{3/2}(N+1)^3 \lambda}{(n'^2 + m'^2)^{3/2}}.$$

For $n' \leq N$ and $m' \leq N$, we use the crude estimates

$$\frac{1}{(n'-n)^2 + (m'-m)^2} \leq 1$$

and

$$1 \leq \frac{2N^2}{n'^2 + m'^2}.$$

Thus we have

$$|f_{n'm'k'}^{(s)}| \leq \frac{a^s C^{s-1} 2^{3/2} N^3 \lambda}{(n'^2 + m'^2)^{3/2}}.$$

By denoting $C = 2^{3/2}(N+1)^3 \lambda$, Eq. (A4) is satisfied for all n, m and for all s.

It follows that for $a < 1/C$, the same inequality holds for f:

$$\langle f_{nmk} \rangle \leq \frac{C_\infty}{(n^2 + m^2)^{3/2}},$$

where $C_\infty = a^2 C^2/(1-aC)$.

---

[1] R. Lima and M. Pettini, Phys. Rev. A **41**, 726 (1990); Int. J. Bifurcation Chaos Appl. Sci. Eng. **8**, 1675 (1998); L. Fronzoni, M. Giocondo, and M. Pettini, Phys. Rev. A **43**, 6483 (1991).

[2] G. Chen and X. Dong, Int. J. Bifurcation Chaos Appl. Sci. Eng. **3**, 1363 (1993).

[3] J. R. Cary, Phys. Rev. Lett. **49**, 276 (1982); J. D. Hanson and J. R. Cary, Phys. Fluids **27**, 767 (1984); J. R. Cary and J. D. Hanson, *ibid.* **29**, 2464 (1986); C. C. Chow and J. R. Cary, Phys. Rev. Lett. **72**, 1196 (1994); W. Wan and J. R. Cary, *ibid.* **81**, 3655 (1998); S. R. Hudson, D. A. Monticello, A. H. Reiman, A. H. Boozer, D. J. Strickler, S. P. Hirshman, and M. C. Zarnstorff, *ibid.* **89**, 275003 (2002).

[4] Y. C. Lai, M. Ding, and C. Grebogi, Phys. Rev. E **47**, 86 (1993); Y. C. Lai, T. Tél, and C. Grebogi, *ibid.* **48**, 709 (1993); O. J. Kwon, Phys. Lett. A **258**, 229 (1999); Y. Zhang and Y. Yao, Phys. Rev. E **61**, 7219 (2000); B. Doyon and L. J. Dubé, *ibid.* **65**, 037202 (2002).

[5] Y. Zhang, S. Chen, and Y. Yao, Phys. Rev. E **62**, 2135 (2000); J. H. E. Cartwright, M. O. Magnasco, and O. Piro, *ibid.* **65**, 045203(R) (2002).

[6] G. Gallavotti, in *Regular and Chaotic Motions in Dynamical Systems*, edited by G. Velo and A. S. Wightman (Plenum, New York, 1985); Commun. Math. Phys. **87**, 365 (1982); G. Gentile and V. Mastropietro, Rev. Math. Phys. **8**, 393 (1996).

[7] H. Xu, G. Wang, and S. Chen, Phys. Rev. E **64**, 016201 (2001); J. Gong, H. J. Wörner, and P. Brumer, Phys. Rev. E **68**, 056202 (2003).

[8] A. Oloumi and D. Teychenné, Phys. Rev. E **60**, R6279 (1999).

[9] C. D. Schwieters and H. Rabitz, Phys. Rev. A **44**, 5224 (1991); J. Botina, H. Rabitz, and N. Rahman, *ibid.* **51**, 923 (1995); E. M. Bollt and J. D. Meiss, Physica D **81**, 280 (1995); Phys. Lett. A **204**, 373 (1995).

[10] Z. Wu, Z. Zhu, and C. Zhang, Phys. Rev. E **57**, 366 (1998); L. Sirko and P. M. Koch, Phys. Rev. Lett. **89**, 274101 (2002).

[11] M. Pettini, A. Vulpiani, J. H. Misguich, M. De Leener, J. Orban, and R. Balescu, Phys. Rev. A **38**, 344 (1988); M. Pettini, in *Non-Linear Dynamics*, edited by G. Turchetti (World Scientific, Singapore, 1989).

[12] B. D. Scott, Phys. Plasmas **10**, 963 (2003) and the list of references [3] therein.

[13] A. J. Lichtenberg and M. A. Lieberman, *Regular and Stochastic Motion* (Springer-Verlag, Berlin, 1993).

[14] A. Crisanti, M. Falcioni, G. Paladin, and A. Vulpiani, La Rivista del Nuovo Cimento **14**, 1 (1991); T. Bohr, M. H. Jensen, G. Paladin, and A. Vulpiani, *Dynamical Systems Approach to Turbulence* (Cambridge University Press, Cambridge, 1998); M. Hénon, C.R. Acad. Sci. Paris A **262**, 312 (1966).

[15] R. McWilliams and M. Okubo, Phys. Fluids **30**, 2849 (1987).

[16] Ph. Ghendrih, Y. Sarazin, G. Attuel, S. Benkadda, P. Beyer, G. Falchetto, C. Figarella, X. Garbet, V. Grandgirard, and M. Ottaviani, Nucl. Fusion **43**, 1013 (2003).

[17] JET Team, Nucl. Fusion **39**, 1891 (1999).

[18] T. J. Northrop, Ann. Phys. (N.Y.) **15**, 79 (1961).

[19] E. Amato, M. Pettini, and M. Salvati, Astron. Astrophys. **402**, 819 (2003).

[20] M. Vittot, J. Phys. A (to be published), e-print math-ph/0303051.

[21] A. J. Wootton, H. Matsumoto, K. McGuire, W. A. Peebles, Ch. P. Ritz, P. W. Terry, and S. J. Zweben, Phys. Fluids B **2**, 2879 (1990).

[22] M. Guzzo, E. Lega, and C. Froeschlé, Physica D **163**, 1 (2002).

[23] G. Ciraolo, C. Chandre, R. Lima, M. Vittot, and M. Pettini, Cel. Mech. Dyn. Astr. (to be published), e-print nlin.CD/0311009.

[24] G. Ciraolo, C. Chandre, R. Lima, M. Vittot, M. Pettini, C. Figarella, and P. Ghendrih, J. Phys. A **37**, 3589 (2004).